Mapping of submerged aquatic vegetation in rivers from very high-resolution image data, using object-based image analysis combined with expert knowledge

Mapping of submerged aquatic vegetation in rivers from very high resolution image data, using Object Based Image Analysis combined with expert knowledge

Fleur Visser[1]*, Kerst Buis[2], Veerle Verschoren[2], Jonas Schoelynck[2]

Affiliations+ addresses of authors:

1) Institute of Science and the Environment, University of Worcester, Henwick Grove, Worcester WR2 6AJ, UK

2) Department of Biology, Ecosystem Management Research Group, University of Antwerp, Universiteitsplein 1C, B–2610 Wilrijk, Belgium;

Contact details corresponding author:

*f.visser@worc.ac.uk; Tel.: +44-1905-855236.

Abstract

The use of remote sensing for monitoring of submerged aquatic vegetation (SAV) in fluvial environments has been limited by the spatial and spectral resolution of available image data. The absorption of light in water also complicates the use of common image analysis methods. This paper presents the results of a study that uses very high resolution (VHR) image data, collected with a Near Infrared sensitive DSLR camera, to map the distribution of SAV species for three sites along the Desselse Nete, a lowland river in Flanders, Belgium. Plant species, including *Ranunculus peltatus*, *Callitriche obtusangula*, *Potamogeton natans*, *Sparganium emersum*, and *Potamogeton crispus*, were classified from the data using Object-Based Image Analysis (OBIA) and expert knowledge. A classification rule set based on a combination of both spectral and structural image variation (e.g.

texture and shape) was developed for images from two sites. A comparison of the classifications with manually delineated ground truth maps resulted for both sites in 61% overall accuracy. Application of the rule set to a third validation image, resulted in 53% overall accuracy. These consistent results show promise for species level mapping in such biodiverse environments, but also prompt a discussion on assessment of classification accuracy.

Keywords

Macrophytes; OBIA; Remote Sensing; VHR image data; knowledge-based

INTRODUCTION

Until recently remote sensing has rarely been used as tool for monitoring of submerged aquatic vegetation (SAV) in fluvial environments. This is partly due to the limited spatial resolution of image data produced by conventional sensor/platform combinations. Another problem is the absorption of light in water, particularly in wavelengths most suitable for vegetation detection, which complicates the use of common image analysis methods (Lucas and Goodman, 2014). Several recent technological developments are now enabling researchers to overcome some of these issues. Firstly the rapid development in remote sensing platforms such as Unmanned Aerial Systems (UAS) now allows collection of very high resolution (VHR) image data of (sub-)centimetre resolution with wavelength bands beyond the visible light (e.g. Lucieer et al., 2014). In addition to this the relatively new Object Based Image Analyis (OBIA) approach can be used to derive information from images, while relying less on spectral information only (e.g. Laliberte et. al, 2011).

The OBIA method works by first segmenting an image into objects that consist of groups of spectrally similar and adjacent pixels, rather than classifying an image on a pixel by pixel basis. The objects formed this way will vary in shape and size, depending on the underlying image and the segmentation algorithm used, and therefore provide an extra spatial dimension to the data, which can benefit image interpretation. The approach works particularly well in combination with VHR image data, which is now more commonly available (Blaschke, 2010). A close up of a river section with two different

vegetation species (*C. obtusangula* and *R. peltatus*) shown in Figure 1, helps illustrating the advantage of OBIA compared with pixel-based image analysis. Due to the variable, but comparable spectral values of the two plants it is difficult to classify individual pixels as belonging to either of the two species. However, a trained observer can readily identify what part of the section is covered in which species, based on additional image detail such as leaf and stem shapes. OBIA can include this kind of contextual information during the object-based image analysis process and therefore seems a promising contribution to the development of an automated detection tool for Submerged Aquatic Vegetation (Visser et al. 2013).

Only recently OBIA is being applied specifically for the detection and classification of SAV. However, these studies are so far mostly undertaken in coastal environments (e.g. Klemas, 2013; Roelfsema et al., 2014) and few involve classification of image data beyond plant functional level (e.g. Dronova et al. 2012). A review of methods used for plant species classification, also showed that few studies make use of VHR images in order to derive specifically geometric attributes of objects to enhance a classification (Dronova, 2015). The authors of this paper argue that classification through knowledge-based rule sets, which exploit such attributes/features, is a particular strength of OBIA and should be explored further. Visser et al. (2013) already showed how the approach can improve SAV detection compared to classification based on spectral information only. With the study presented in this paper we aim to show how a multi-level knowledge-based OBIA can provide a practical approach to map complex SAV communities at species level in a clear water stream.

METHODS

STUDY SITE

Data for this study were obtained from the Desselse Nete, which is a lowland stream in Flanders, Belgium with an average water depth of approximately 0.6-0.7 m, a mean width of 6.2 m and a mean discharge of 0.3- 0.6 $m^3 s^{-1}$. The river has generally low suspended solid and organic matter concentrations (<50 mg/l). Three river sections of approximately 5 x 5 m length were selected close to

its confluence with the Zwarte Nete near the village of Retie. Data were collected in May 2012, when the vegetation on one sample site consisted of dense submerged patches of Pond Water Crowfoot (*Ranunculus peltatus*), Blunt-fruited Water Starwort (*Callitriche obtusangula*) and Curly-leaf Pondweed (*Potamogeton crispus*). The plants on two other sample sites were more open and consisted of Broad-Leaved Pondweed (*Potamogeton natans*), and European Bur-reed (*Sparganium emersum*).

IMAGE DATA ACQUISITION

The specific advantages of OBIA can only be deployed in analysis of images with sufficient detail (Blaschke, 2010). The method therefore works best on VHR image data. An increasingly popular type of platform from which to obtain such data is an unmanned aerial system (UAS) (Anderson & Gaston, 2013; Woodget et al., 2015). Data collection from UAS-s is however still constrained by issues such as weather conditions and the short battery life of many systems. Alternative ground-based platforms such as telescopic poles, are gaining popularity too and are not affected by such issues (e.g. Hauet et al., 2009; Laliberte et al.,2007; Luscier et al., 2006; Visser et al., 2013), however their application is limited by the spatial extent of images obtained from lower altitudes. For the current project spatial extent was not a prerequisite, so image data was collected from a telescopic pole fixed in position with guy ropes at approximately 4.5 m at nadir over the centre line of the river.

Earlier research has indicated the importance of near infrared (NIR) light reflectance for the detection of SAV in shallow submerged environments (Visser et al., 2013). We therefore collected both colour photographs (RGB) and single band NIR photographs. The photos were obtained with a Fujifilm IS-Pro NIR sensitive digital single-lens reflex (DSLR) camera and a Tamron AF Aspherical 28-80 mm f/3.5-5.6 lens. This camera model does not contain any internal NIR or ultraviolet (UV) blocking filters and therefore senses the full spectrum of UV, visible light (VIS) and NIR light. By adding different filters to the lens, selected parts of the electromagnetic spectrum can be captured by the camera sensor. Red, Green and Blue image bands were obtained by adding a NIR blocking filter (model XNite CC1, LDP LLC, Carlstadt, USA, formerly ‘maxmax.com’, here referred to as ‘CC1’), which transmits only VIS light, while using all three RGB senor channels. A single band covering most of the NIR spectrum (NIR(R72)) was obtained by adding a Hoya R72 VIS blocking filter to the

lens. A further two bandpass filters (XNite Bandpass IR Filters, LDP LLC, Carlstadt, USA), were used to obtain one narrow NIR wavelength band around 710 nm (model XNite BPB, here referred to as 'NIR (BP1)') and one around 828 nm (model XNite BPG, here referred to as 'NIR(BP2')). Figure 2 shows the filter transmission spectra.

The Fujifilm IS-Pro was used in combination with a radio controlled shutter and produced photos of 3024x2016 pixels in 8-bit GEOTIFF format. Although RAW is seen as the preferred image format for image analysis (Verhoeven, 2010) TIFF was chosen in this study because of its ease of use (format and file size). Relative ambient light conditions were estimated with an ATP DT-1309 Auto Ranging Light Meter.

IMAGE PRE-PROCESSING

RADIOMETRIC DATA ISSUES

Due to the low altitude of the sensor platform atmospheric correction of the image data was not needed. However, several other types of radiometric issues clearly affected the acquired image data, which were sunglint, skyglint and specular reflection at the water surface, as well as shadows from surrounding vegetation and hotspotting effects caused by the camera. Several methods exist in the literature for removal of sunglint, however they were mostly developed for marine environments and therefore not really suitable for small scale, shallow river environments (Kay et al., 2009; Visser et al., 2015). In this study objects affected by glint were assigned to a separate class during rule set development and that way excluded from further analysis. The authors of this paper are not aware of effective methods that can be used to remove skyglint, specular reflection at the water surface, nor for the removal of significant shadow effects. No attempts were therefore made to remove/reduce their effect.

Concentric bands of lighter shades that occur in some of the NIR(BP2) images were thought to be so called 'hotspotting' or 'lens flaring'. This radiometric anomaly occurs due to internal reflection of light between the camera, lens and possible filters and is quite commonly observed in NIR photography (Verhoeven, 2008). Its occurrence is camera, lens, filter, light and aperture dependent

and therefore not easy to predict and avoid. Visser et al. (2015) attempted to remove the effect with and image based correction method. For their study the improvement was visible but had insignificant effect on the overall results.

In summary, as known correction approaches did not seem to significantly improve image quality, no radiometric pre-processing steps were undertaken before image analysis. The effect this may have had on the classification results are considered in the Discussion section.

Geometric Correction

Geometric correction of digital photographs usually involves a lens barrel correction, however, no lens profile data was found for the Tamron lens used in this project. An alternative distortion assessment on geometry in sample photographs, using Adobe Photoshop did not indicate significant distortion in horizontal or vertical direction, confirming claims of Tamron (tamron-usa.com) that this type of 'AF Aspherical' lens, eliminates aberrations and distortion. No correction was therefore applied to the photos before undertaking further analysis.

To align all photos co-registration was undertaken using four fixed ground control points that were included in all photos, as well as additional features that could be identified in multiple photos. Second order polynomial transformations were applied to match the photographs, which resulted in root mean square errors (RMSE) of 0.1 to 10 cells ((≈ 0.2 to 24 mm). Some of the larger errors would have been caused by lack of matching tie points within the scene in addition to the four ground control points. Finding identical features in the moving water and on the grassy banks proved extremely difficult. The transformed data was resampled using the Nearest Neighbour algorithm, to produce final image layers. Three single band NIR and one RGB colour images were combined into a multi-band image file and cropped to remove parts of the scene not covered by all four images.

Object Based Image Analysis

The most commonly used image classification algorithms work on a pixel-by-pixel basis, where the spectral values of a pixel are used to assign that pixel to the most suitable class. By first grouping adjacent pixels with similar spectral values into objects (the segmentation process) and including

features of those objects in the image classification process, classifications can be significantly improved (Blaschke et al., 2011). Object features can be spectral values, representing average object reflectance as well as within-object reflectance variability, but also geometric features such as shape (e.g. roundness or length/width ratio), or internal texture and relationships to adjacent objects (e.g. contrast to neighbouring object). Classifying an image using rule sets based on such feature values, may better replicate the perception of an expert in the field (e.g. Blaschke, 2010; d'Oleire-Oltmanns et al., 2014). These and other different theoretical foundations of OBIA compared to the 'per-pixel' approach are believed to be a new paradigm in remote sensing and GIS science (Blaschke et al., 2014).

For this study we selected two of the three sites to develop a classification rule set. Selection was based on the range of vegetation types present at each site, as the validation site should not contain any species that were not present at the sites used for rule set development. The sites used for rule set development are referred to as site 1 and 2. The final rule set was then applied to the image of the third site, site 3, to test its transferability. All three classified images were compared with manually obtained reference images to assess the performance of the rule set. Further details on each of these OBIA analysis steps are given in the following sections.

IMAGE SEGMENTATION

In this project we used multiresolution segmentation as available in eCognition Developer software (Trimble Geospatial), with which objects can take on any form during the segmentation process. The shape and size of the objects are to some extent constrained by three parameters that can be set before running the segmentation. These are scale, shape and compactness. A segmentation can be based on the spectral values in all image data layers combined. In our analysis we applied segmentation to one image data layer only, rather than a combination of the six available layers. The NIR(BP1) layer was selected for this purpose, as it was noted by the experts involved that this layer allowed best identification of SAV species, and therefore thought to result in most relevant object delineation. The decision to use a single band for segmentation was determined by the limitations of our equipment, which did not allow for simultaneous collection of all image bands. In combination with the dynamic

nature of the submerged vegetation this meant that plant elements such as leaves were not located in exactly the same position in each image data layer and thus would not show up as distinct objects during a segmentation based on multiple layers.

Segmentation was performed at two different levels. Each level had a clear target object size. At Level 1 we aimed to delineate objects of the size of individual patches of plant species. At Level 2 we aimed to delineate smaller objects representing plant morphological elements such as individual leaves and stem segments. The most suitable scale parameter for each level was determined by trial and error. Quite recently tools have been developed to automatically identify meaningful parameter values (e.g. Drăguţ et al., 2010), but mostly for scenes where there is no a priori knowledge of meaningful object scales. In this study we were able to identify meaningful objects based on expert knowledge of plant morphology prior to the OBIA analysis. Suitable scale parameter values where therefore obtained by running segmentations with different parameter settings and choosing those that provided the best results according to the expert's judgement. The chosen parameter values and settings for each of the two segmentation levels are as follows:

Level 1: Multiresolution segmentation: Scale parameter 100; Shape 0.2 Compactness 0.2: NIR(BP1) data layer only.

Level 2: Multiresolution segmentation: Scale parameter 20; Shape 0.2 Compactness 0.2: NIR(BP1) data layer only.

The same values were applied to the images of each of the three sites.

CLASSIFICATION RULE SET DEVELOPMENT THEORY

After the image is segmented into image objects, the next step is to classify these objects in to the correct class of a predefined class hierarchy. In our project the class hierarchy consisted of the species as observed in the river sections, plus a bottom, an emergent vegetation, and some mixed vegetation classes. There are many different ways in which a rule set for the object classification can be developed. Some authors have used supervised classification approaches similar to those used in

pixel-based image analysis, where samples of objects are used to produce statistical class descriptions according to which the remainder of the objects can be classified (e.g. Mui et al., 2015; Roelfsema et al., 2014). However, one of the great advantages of OBIA is its suitability for knowledge based/driven rule set development. In this study we particularly wanted to replicate some of the cognitive steps undertaken by SAV experts in order to identify vegetation species from aerial photographs. Significant advances have been made organizing and expressing domain knowledge into a machine-readable format (Belgiu et al., 2014), but this approach is very much 'work in progress', so in this study we have limited ourselves to expert rule set development using a trial and error approach (e.g. Rampi et al. 2014) to test what kind of accuracy can be achieved this way. An important disadvantage of this approach is the level of subjectivity and the relatively time consuming practice of manually developing the rule set. A satisfactory result that proves to be transferrable and can be used to map SAV over a much wider area would however strongly compensate for these shortcomings.

When deciding on rules and thresholds we aimed to select mostly features that would be least affected by changes in image resolution and illumination conditions. Spectral object feature values used in the classification were derived from individual image data layers as well as from combinations of layers. It appeared however impossible to create an effective rule set without the use of thresholds involving absolute spectral values from some (combination) of the six image data layers (i.e. red, green, blue, NIR(BP1), NIR(BP2) and NIR(R72)), so they were included where needed. The effect this has on transferability of the final rule set will be addressed in the Discussion section. Image scale will also affect the effectiveness of class rule thresholds, as the size and shape of an object determines the number and location of pixels included and consequently the overall object values (Li and Shao, 2014). Since photos for all three sites were taken from very similar elevations, we expect the same optimal scale parameter values to apply. For all types of features we have optimized class rule thresholds manually through an iterative process of modifying thresholds and observing the classification results for the two 'training' images simultaneously.

RULE SET DEVELOPMENT STEPS

The flow diagram of Figure3 shows how all objects were classified according to a predefined class hierarchy, by means of a set of rules. The rules applied for each class are listed in Table 1. In the table classes as used in the final SAV species maps are indicated with an 'f'. A number of intermediate (temporary) classes, usually consisting of a combination of species, were also created during the process. They are listed in the table with a 't'. For some classes all objects were assessed while for other classes only objects previously assigned to another (temporary) class are considered. The structure of this process is indicated with flow lines in Figure 3. Classes created at different segmentation levels are separated in the diagram and flow lines indicate where Level 2 classes (L2) are used as input for Level 1 classification (L1). A detailed motivation for the choice of features used for the classification rules for each class is given below. Where multiple levels are used to identify a target surface/species, this is mentioned in the motivation:

Bank vegetation and exposed macrophytes (f, L1) – NIR reflectance of SAV is more strongly absorbed than VIS reflectance due to the overlying water column. This effect is absent from emergent and terrestrial vegetation. NDVI is a feature commonly used in remote sensing to differentiate vegetated from non-vegetated surfaces. In a similar way this feature allows for separation between emergent and submerged vegetation. As its value is made up of a ratio of image bands it can be considered a relative spectral measure. NDVI values are negative for all aquatic classes while emergent and terrestrial vegetation have positive values. NIR(R72) has the strongest reflectance for emergent and terrestrial vegetation, which makes the mean of this band useful for separation from submerged aquatic vegetation.

Bottom (f, L1) – Parts of the images representing the river bed generally have very low reflectance values, particularly in the longer wavelength NIR band (i.e. NIR(BP2)), therefore a threshold value for this band was selected. This type of surface also tends to be very homogeneous, compared to other surfaces, particularly in the NIR(R72) band. The standard deviation for this band is therefore selected as a second selection criterion for bottom objects.

C. obtusangula/*R. peltatus*/*P. crispus* (t, L1) – These three species all seem to reflect particularly strongly in the NIR(BP1) band, so this band is used to seperate objects that definitely aren't either of these species (i.e. low NIR(BP1)).

P. crispus (f, L1) – This plant has a curly leaf, which is most distinct in the NIR(BP1) band where the undulating leaf surface creates clear spectral contrast, which can be quantified by means of the standard deviation of this feature.

P. natans (f, L1+L2) – The most distinct characteristic of the *P. natans* plant are its floating oval shaped leaves. At the Level 2 segmentation these leaves are delineated and can be classified through a combination of rules relating to the object roundness; area (<450 pxl); 90 < Brightness < 134; Their relatively short length (< 50 pxl); a specific length/width ratio and a distinct difference in colour to neighbouring object, particularly in band NIR(BP1) < 4. Brightness is calculated as the 'mean value of the spectral mean values of an image object' (Definiens AG, 2007).

S. emersum (f, L1+L2) – The leaves of this plant are very narrow and highly reflectant, which enables delineation and classification at the level of individual leaves. Features used are length/width ratio, absolute width, relative border to brighter objects in NIR(BP1). The latter feature represents the length of the shared border of neighbouring image objects with a higher brightness value. Also the absolute mean value of NIR(BP1) is used, as this is the layer in which the objects show up clearest.

S. emersum - *P. natans* Mix (f, L1) – Due to the nature of these two species they locally form a very homogeneous mixture, which makes it nearly impossible to separately map each species. For these situations a separate mixed class has been allocated, which is dependent on the presence of a minimum number/area cover of sub objects for each of the two species.

C. obtusangula / *R. peltatus* (t, L1) – Objects that potentially are *C. obtusangula* or *R. peltatus* are assigned to this temporary class based on the shape of their sub objects and reflectance in the red band.

C. obtusangula (f, L1+L2) – This plant has distinct rosette shaped leaves, which are delineated as round/square objects at Level 2 with a particularly low length/width ratio (<2). The actual plant objects at Level 1 can be identified by the relative area taken up by the rosettes, in combination with the absence of Level 2 *P. natans* leaf sub-objects. Only objects previously classified as *C. obtusangula* / *R. peltatus* / *P. crispus* are used as input.

R. peltatus (f, L1+L2) – This species can be recognised in photos by its highly reflectant stem surrounded by furry leaves. The number of elongated leaves/stems is used to separate *R. peltatus* objects from the *C. obtusangula* / *R. peltatus* / *P. crispus* class.

Sunglint (f, L1) – Sunglint shows in the image as white light, which means high values in all three visible image bands. The intensity of these three bands combined is represented by the Brightness value. A high threshold of 160 effectively classifies all sunglint objects. Some exposed surfaces with similar brightness values, were previously classified as exposed and therefore excluded from this step.

Exposed bank/Oats on bed (f, L1) – Soil, as visible at exposed banks, has a distinct high red reflectance, which is a common characteristic. This class also included patches of oats deposited on the river bed after flow velocity assessments using oat particles, which took place during the same field data collection campaign. The spectral characteristics of the oats were similar to those of exposed soil.

Vegetation general (f, L1) – Of the temporary class *C. obtusangula/R. peltatus/P. crispus* (t, L1) objects that were not redistributed to other classes were classified as 'Vegetation general' as they were thought to be some form of vegetation that could not be identified in more detail through rules. This class was not used in the manually obtained reference maps, as experts were able to identify dominant species cover for all polygons.

Bar (f, L1) – The metal bar across the river which is visible in the image of site 2, could be classified effectively based on the extremely elongated shape of the polygons it is made up of.

COMPARISON OF CLASSIFICATION RESULTS WITH MANUALLY DERIVED SAV MAPS

The reliability of the knowledge-based OBIA approach was assessed by comparing the classification results for each of the three sites with maps, in which vegetation classes have been manually delineated. For remote sensing classification studies accuracy assessments are usually done by taking a sample of pixels from across the classes represented in the image. Based on this sample an error matrix is calculated, from which then an overall accuracy and kappa coefficient are calculated. The former is the percentage of correctly classified pixels and latter coefficient supposedly provides a similar measure, but adjusted for agreement occurring by chance. Although still commonly applied, the usefulness of the kappa coefficient has recently come under debate (Olofsson et al., 2014) and is there for not used in this paper. For OBIA classifications it is generally accepted that the sampling units should consist of polygons rather than pixels (Radoux et al., 2011), however a universally accepted method to compare classification and reference polygons when they can differ both in size and class definition, has not yet been devised. A slightly exceptional situation in this study occurred due to the fact that the manually obtained reference data covers the full classification area, which means a direct comparison between the two data layers can be made and no inferential statistics is needed to estimate the accuracy of the classification. When doing a comparison based on polygon units however, a problem could still arise, as the automatic classification polygons would not necessarily line-up with the manually delineated polygons, which would result in positional as well as thematic differences and are difficult to tackle simultaneously. Instead we decided to create a manual reference layer by using the Level 1 segmentation polygons and manually classify each polygon, referring to each of the six image data layers for confirmation, as well as to overview sketches of the patch distribution and species composition, which were made in the field.

During the classification process it was observed that some polygons were undersegmented as these polygons clearly consisted of more than one class, which dominated in distinctly different parts of the polygon. For such polygons an expert would have decided to separate the classes with an additional boundary, but this was not possible due to the segmentation framework. In these situations the polygon was given the class value of the most dominant species appearing in that polygon. Where species cover was too low or too difficult to distinguish, the polygons were classed as Bottom.

To evaluate the transferability of our approach we were particularly interested to see how similar the validation classification of site 3 is to the manual map of site 3 compared to the comparisons for the two sites, used for rule set creation.

RESULTS

Figure 4 shows close-ups of the Level 2 segmentation and classification, as used in the image analysis procedure. Figures 5-7 show the final classification results for each of the three sites, together with the manually delineated class maps, as well as the NIR(BP1) image source data layer. The classification results clearly bring out the different composition of the vegetation communities found at each of the sites as, well as the more mixed cover type found on site 3.

The overall accuracy coefficient shows the agreement between the OBIA–derived classification map and manual reference data (Table 2). The coefficient is highest for the classification of site 1and lowest for that of site 3. All values are below what is generally seen as an acceptable level of accuracy for an image classification even compared to other studies undertaken under the challenging conditions provided by submerged aquatic environments (Dronova, 2015; Husson et al., 2014). Looking at the classification accuracies for individual species (Table 3) they vary between sites. User's and producer's accuracies (UA and PA) are the best measures to evaluated these. For example the classification of bottom for site 1 has a very high UA (0.98), meaning that there is a high likelihood that an automatic classification result corresponds with the reference map. Looking however at the PA this is considerably lower (0.69), because many of the bottom polygons on the reference map have not been correctly classified by the automatic classification. When assessing all other classes in a similar way some classes perform better than others. The class 'Bank vegetation and exposed macrophytes' seems to be classified best as for all three sites both the UA and PA are amongst the top three highest, with values ranging between 0.70 and 0.93. Bottom also seems well classified, for site 1 and 2 (0.69 to 0.98), but both UA and PA are low for site 3 (0.57 and 0.29). For the latter site bank and bottom are often misclassified as vegetation general and several polygons were classified by the expert as glint, but by the algorithm as bottom. Consequently glint has a very low PA

for this site (0.28). At site 2 this class performs better, with almost 100% accuracy, while at site 1 glint is classified by the algorithm but not observed by the expert. The best performing vegetation species is *P. crispus*, but this species was only observed at site 1 (UA = 0.50 and PA = 0.64). *C. obtusangula* only occurs on site 1 (UA = 0.5 and PA = 0.76) and 3 (UA = 0.44 and PA = 0.47). For both sites most confusion occurs with *R. Peltatus.* In the mixed class most confusion occurs with the pure *P. natans* and *S. emersum* as could be expected since that is what the mix consists of. The pure *P. natans* and *S. emersum* classes have reasonable UAs and PAs ranging between (0.41 and 0.68) for site 2 and 3, but lower ones for site 2 where the values are highly variable (between 0.00 and 0.5). This is most likely due to the absence of the species there resulting in a low number of misclassifications which leads to low UA an PA values. At site 1 where *R. peltatus* was most dominant the UA for this species was high (0.82), however many patches identified by the expert were misclassified as bank, vegetation general or *S. emersum* resulting in a PA of only 0.29. The species did not perform any better on the other sites (UA and PA between 0.67 and 0.11). The class vegetation general picked up polygons that did not fit in any of the other (vegetation) classes. Across all sites in particular polygons classified as bottom by the expert ended up in this class, but also *R. peltatus, P. natans* and the mixed class were misclassified. .

DISCUSSION

CLASSIFICATION ACCURACY

The results of this study show that OBIA has potential to aid mapping of SAV in clear-water streams. The most promising result is a rather consistent overall accuracy of 53-61% for both the sites used in the development of the classification rule set and the validation site. Although for remote sensing classification studies an overall accuracy >85% is generally set as a target level, this is rarely attained (Foody, 2012) and these standards have been devised for terrestrial environments that do not suffer from complicating factors experienced in aquatic environments, such as absorption of light by water. So despite the relatively low similarities between the OBIA classification and the manually produced

maps we consider the results as promising with more than half of each image correctly classified. In particular because a single rule set was used to achieve this, we think it is an acceptable result that warrants further investigation of the approach.

Considering only those vegetation classes that were observed by the expert at either site, it is difficult to find one or more that consistently perform worst. There also do not seem to be any very consistent confusions/misclassifications. This makes it difficult to provide useful recommendations on how the rule set may be modified to improve the results. The use of multi-level classification and segmentation, which identified specific plant morphological elements shows promise to tackle such canopy complexity, however, further research is needed to identify the most appropriate rules that can characterise/formalize boundaries within and between patches of mixed vegetation. Furthermore some very deep *S. emersum* and *P. natans* was identified by the expert, but appeared not sufficiently distinct to be included in the segmentation and classification as distinct objects/patches, which will have influenced the accuracy results. Further gains in improvement of the classification probably require improvement of the data quality as will be discussed in the following sections.

IMAGE DATA QUALITY

An important factor that needs to be considered when evaluating the classification results is the quality of the image data used. In this case image data was collected with a consumer-grade digital camera and a set of separate filters. The various image layers used in the analysis were therefore not collected simultaneously. As a result the image elements such as individual plant leaves are not in exactly the same location in four of the six bands used, due to movement of the plants with the river current. This will have significantly affected the image segmentation and the effectiveness of certain rules used. All segmentation was done on one layer only, while rules were developed using multiple layers as well as different individual layers. For example one of the rules used to create the temporary class '*C. obtusangula / R. Peltatus*', is based on a range of values for the mean red band. It is very likely that this rule would be more effective if plant leaves and stems in the red band would be positioned in exactly the same location as in the NIR(BP1) band and thus line up exactly with object boundaries. Data collected with a multi-spectral optical sensor of sufficient spatial and spectral

resolution will therefore most likely result in a significant increase in classification accuracy. The advantage of the method demonstrated here is however its cost effectiveness and relatively low weight. It is possible for one person to carry the set up applied here (or to attach to an UAS) and that way collect images over much larger areas (Verschoren et al. This issue).

A number of different factors affected the radiometric values of the image data, including sunglint skyglint, specular reflection, hotspotting and shading. Sunglint was effectively identified during the image classification process for site 2 (PA = 0.80 and UA 1.00), though slightly less well site 3 (PA = 0.28 and UA = 0.78). These results suggest that by applying a classification rule glint-affected objects can be identified and eliminated during further application of the classification results. Information of vegetation cover is however lost for these locations, so final cover maps would involve interpolation of some kind. The presence of adjacency effects such as the reflection of vegetation at the water surface is particularly strongly visible in the NIR and may have influenced the segmentation based on the NIR(BP1) band. Until an effective way has been developed to remove/avoid such effects, this will remain a significant issue for remote sensing in river environments where the distance between any part of the water surface and surround terrestrial vegetation is generally small. Since the flaring/hotspotting effect only occurred in band NIR(BP2) it did not show up in the segmentation patterns and as this band was not often selected as feature in classification rules we expect that it had little or no effect on the classification results. Pre-processing to remove this effect is deemed unnecessary. Photos for this project were collected under suboptimal conditions and some are therefore affected by skyglint and/or shading. These effects were not clearly visible in the delineation of image segments, but may have affected the effectiveness of rules based on absolute spectral values. Ideally these kinds of effects should be reduced by choosing the right time of the day and clear sky conditions for image data collection. This is however not always achievable due to time constraints on data collection, as was the case with this project. The occurrence of skyglint and/or shading will affect most types of remote sensing, however, because of its reduced reliance on spectral information, the OBIA method proposed here may actually be relatively insensitive to these kind of issues.

Another important factor that will affect the collection of images of sufficient quality and has influenced the presented results to some extent, is its reliance on clear and shallow waters. This is a universal issue affecting the application of optical remote sensing approaches in aquatic environments. In our classification we experienced difficulties delineating and classifying the deeper vegetation patches. Shallow water is however the environment where the method would be of most benefit, as this is where the greatest diversity of SAV can be expected, so there will be a sufficiently large environment for which the method can be very suitable. Finally the current resolution and 2D nature of most remote sensing data does not provide enough detail to enable assessment of the large amount of morphological variation that can be found amongst certain SAV species, making them nearly impossible to identify. Where these boundaries for SAV classification lie requires further investigation.

APPLICATION POTENTIAL

The fact that one rule set was created, which consistently performed moderately well on three rather different scenes suggest that this approach may be transferable and allow rapid mapping of SAV communities on larger scales in similar river environments. There is significant room to improve the classification results, as the overall accuracy values where not high. However, we think the performance of the classification rule set should be seen in the light of the specific complications of the submerged aquatic environment for which the classification was performed, complex mixtures of vegetation species present in the three images, as well as the image data quality issues discussed above. We therefore recommend that the approach is investigated more widely in order to further explore its potential.

Although the authors tried to avoid using absolute spectral values, which are directly dependent on changes in illumination conditions in an image, it appeared not possible to fully achieve this. With changes in illumination conditions or similarly changes in water transparency thresholds based on these values, will need to be adjusted. By including such thresholds as variables within the rule set, they can easily be adjusted by adaptation of the master rule set and so avoiding having to develop rule sets from scratch (Tiede et al. 2010). In similar ways adaptations to the rule set can be made to

compensate for changes in scale with changes in elevation of the camera used, which will affect features based on (absolute) size and shape values. Also a more automated/objective object scale parameter optimization, similar to the method used by Anders et al. (2011) may make the OBIA approach more robust.

When the rule set proves sufficiently robust over space and time the process can easily be scaled up and is only limited by the ability of a researcher to collect photographs of sufficient resolution. With currently available quality of digital cameras, photos will still have to be collected from relatively low altitude, which results in relatively small image footprints (app. 5 x 5 m). Only suitable platforms for data collection are therefore telescopic masts/poles or rotary winged UAS-s that can operate sufficiently close to the water surface. Rapid sensor development is likely to remove this limitation in the near future. Considering the relatively low dimensionality of the image data (app. < 6 image bands) data volume is thought not to be a problem.

The rule-based classification using expert knowledge is relatively intuitive and can be made accessible to and can be amended by people without remote sensing expertise. It is even highly recommendable to discuss image classifications with aquatic plant experts as their knowledge and cognitive processes to recognize submerged plant species can be used in the classification rule development process. Using the software to write the rule sets and execute the classification does however involve a steeper learning curve and will still require assistance of a remote sensing specialist.

PROGRESS IN KNOWLEDGE BASED CLASSIFICATION

As mentioned by Tiede et al. (2010:194) modelling target classes doesn't just require computational skill, but also a wealth of knowledge 'about the area and the composition of the image setting'. However, as summarized by Arvor et al. (2013), the OBIA knowledge-based approach suffers from various weaknesses, including the 'blackbox' approach of the image segmentation part of the OBIA workflow, but in particular the subjectivity of knowledge and understanding, since all experts have their own conceptualization of the reality they try to map from an image. To resolve the latter issue,

the remote sensing community should therefore endeavour to go beyond this approach and start working with more universal ontologies in combination with tools such as automatic target recognition (ATR) algorithms. Such approaches should be evaluated on their ability to reproduce the reasoning of experts (Arvor, 2013).

Evaluation of many remote sensing based classifications are currently hampered by the availability of reference data. On screen manually delineated classifications/maps are often used for this purpose as they are seen as the most reliable information available. Particularly for SAV, classifications derived manually from remote sensing data are currently the only reliable option available (Husson et al., 2014; Verschoren et al., this issue). However there is reason to question this reliance on manually mapped class boundaries, as they will not be error free, in particular when species form a mixed surface cover as in the current study. There will be a limit to what extent the expert can separate between species, influenced by the time they spend working on the task and their personal concept of reality. We would like to argue that by creating boundaries through a clear set of rules, as is done in OBIA, a more objective interpretation of an image is possible.

CONCLUSION

This paper describes a first attempt at species level classification of SAV, using VHR image data and multi-level knowledge-based OBIA analysis. It demonstrates how VHR image data and the OBIA approach can be used to obtain consistent classifications of submerged aquatic vegetation in shallow clear-water streams using a single object classification rule set The best classification result of 61% overall accuracy slightly less than what has been achieved with more conventional methods such as manual mapping (Husson et al., 2014; Verschoren et al., this issue) or algorithms such as nearest neighbour (e.g. Roelfsema et al., 2014), but need to be seen in the light of the complex study environment as well as the benefit of transferability of the approach

Considering the use of relatively low-tech remote sensing equipment and the sub-optimal conditions during data collection, as well as the heterogeneous vegetation composition of the studied sites, we

think that our results show that OBIA has potential to aid detailed classification of highly biodiverse streams at species level. We even expect that the method can provide an objective quantitative assessment of mixed vegetation cover that may be difficult to map/monitor in other ways. However to confirm this a more detailed comparison needs to be made of the classification accuracy of the OBIA analysis, while providing an assessment of the reliability of the reference data, which presents an interesting challenge in itself.

ACKNOWLEDGMENTS

Funding for this project was provided by the FWO (Fund for Scientific Research) – Flanders (Belgium) – (G.0290.10) via the multidisciplinary research project 'Linking optical imaging techniques and 2D-modelling for studying spatial heterogeneity in vegetated streams and rivers' (Antwerp University, Ghent University, 2010-2013), the FWO Scientific Research Community 'Functioning of river ecosystems by plant-flow-sediment interactions'. V.V. thanks the Institute for the Promotion of Innovation through Science and Technology in Flanders (IWT-Vlaanderen) for personal research funding. J.S. is a postdoctoral fellow of FWO (project no. 12H8616N).

REFERENCES

Agyemang, T.K., J. Heblinski, K. Schmieder, H. Sajadyan & L. Vardanyan, 2011. Accuracy assessment of supervised classification of submersed macrophytes: the case of the Gavaraget region of Lake Sevan, Armenia. Hydrobiologia 661: 85–96. doi:10.1007/s10750-010-0465-7

Anders, N.S., A.C. Seijmonsbergen & W. Bouten, 2011. Segmentation optimization and stratified object-based analysis for semi-automated geomorphological mapping. Remote Sensing of Environment 115: 2976–2985. doi:10.1016/j.rse.2011.05.007

Anderson, K. & Gaston, K. J., 2013. Lightweight unmanned aerial vehicles will revolutionize spatial ecology. Frontiers in Ecology and the Environment, 11 (3), 138–146. doi:10.1890/120150

Arvor, D., L. Durieux, S. Andrés & M.-A. Laporte, 2013. Advances in Geographic Object-Based

Image Analysis with ontologies: A review of main contributions and limitations from a remote sensing perspective. ISPRS Journal of Photogrammetry and Remote Sensing 82: 125–137. doi:10.1016/j.isprsjprs.2013.05.003

Belgiu, M., I. Tomljenovic, T. Lampoltshammer, T. Blaschke & B. Höfle, , 2014. Ontology-Based Classification of Building Types Detected from Airborne Laser Scanning Data. Remote Sensing 6: 1347–1366. doi:10.3390/rs6021347

Blaschke, T., 2010. Object based image analysis for remote sensing. ISPRS Journal of Photogrammetry and Remote Sensing 65: 2–16. doi:10.1016/j.isprsjprs.2009.06.004

Blaschke, T., K. Johansen & D. Tiede, 2011. Object based image analysis for vegetation mapping and monitoring. In Qihao Weng (ed), Advances in environmental remote sensing: Sensors, algorithms, and applications. CRC Press, Taylor and Francis, United States: 141-266.

Blaschke, T., G.J. Hay, M. Kelly, S. Lang, P. Hofmann, E. Addink, R. Queiroz Feitosa, F. van der Meer, H. van der Werff, F. van Coillie & D. Tiede, 2014. Geographic Object-Based Image Analysis – Towards a new paradigm. ISPRS Journal of Photogrammetry and Remote Sensing 87: 180–191. doi:10.1016/j.isprsjprs.2013.09.014

Definiens AG, 2007. Definiens Developer 7 - Reference Book. http://www.ecognition.cc/download/ReferenceBook.pdf

d'Oleire-Oltmanns, S., I. Marzolff, D. Tiede & T. Blaschke, 2014. Detection of Gully-Affected Areas by Applying Object-Based Image Analysis (OBIA) in the Region of Taroudannt, Morocco. Remote Sensing 6: 8287–8309. doi:10.3390/rs6098287

Drăguţ, L., D. Tiede, & S.R. Levick, 2010. ESP: a tool to estimate scale parameter for multiresolution image segmentation of remotely sensed data. International Journal of Geographical Information Science 24: 859–871. doi:10.1080/13658810903174803

Dronova, I., 2015. Object-Based Image Analysis in Wetland Research: A Review. Remote Sensing 7: 6380–6413. doi:10.3390/rs70506380

Dronova, I., P. Gong, N. E. Clinton, L. Wang, W. Fu, S. Qi & Y. Liu, 2012. Landscape analysis of wetland plant functional types: The effects of image segmentation scale, vegetation classes and classification methods. Remote Sensing of Environment 127: 357–369. doi:10.1016/j.rse.2012.09.018

Foody, G.M., 2002. Status of land cover classification accuracy assessment. Remote Sensing of Environment 80: 185– 201. doi:10.1016/S0034-4257(01)00295-4

Hauet, A., Muste, M., Ho, H.-C., 2009. Digital mapping of riverine waterway hydrodynamic and geomorphic features. Earth Surface Processes and Landforms, 34, 242-252.

Husson, E., O. Hagner & F. Ecke, 2014. Unmanned aircraft systems help to map aquatic vegetation. Applied Vegetation Science 17: 567–577. doi:10.1111/avsc.12072

Kay, S., J.D Hedley & S. Lavender, 2009. Sun Glint Correction of High and Low Spatial Resolution Images of Aquatic Scenes: a Review of Methods for Visible and Near-Infrared Wavelengths. Remote Sensing 1: 697–730. doi:10.3390/rs1040697

Klemas, V., 2013. Remote Sensing of Coastal Wetland Biomass: An Overview. Journal of Coastal Research 290: 1016–1028. doi:10.2112/JCOASTRES-D-12-00237.1

Laliberte, A.S., M.A. Goforth, C.M. Steele & A. Rango, 2011. Multispectral Remote Sensing from Unmanned Aircraft: Image Processing Workflows and Applications for Rangeland Environments. Remote Sensing 3, 2529–2551. doi:10.3390/rs3112529

Laliberte, A.S., Rango, A. Herrick, J.E. Fredrickson, E. L., 2007. An object-based image analysis approach for determining fractional cover of senescent and green vegetation with digital plot photography, Journal of Arid Environments, 69 (1), 1–14. doi:10.1016/j.jaridenv.2006.08.016

Lang, S., D. Tiede, D. Hölbling, P. Füreder & P. Zeil, 2010. Earth observation (EO)-based ex post assessment of internally displaced person (IDP) camp evolution and population dynamics in Zam Zam, Darfur. International Journal of Remote Sensing 31: 5709–5731. doi:10.1080/01431161.2010.496803

Li, X. & G. Shao, 2014. Object-Based Land-Cover Mapping with High Resolution Aerial

Photography at a County Scale in Midwestern USA. Remote Sensing 6, 11372–11390: doi:10.3390/rs61111372

Lucas, M. & J. Goodman, 2014. Linking Coral Reef Remote Sensing and Field Ecology: It's a Matter of Scale. Journal of Marine Science and Engineering 3: 1–20. doi:10.3390/jmse3010001

Lucieer, A., Z. Malenovský, T. Veness & L. Wallace, 2014. HyperUAS-Imaging Spectroscopy from a Multirotor Unmanned Aircraft System. Journal of Field Robotics 31: 571–590. doi:10.1002/rob.21508

Luscier, J.D., Thompson, W.L., Wilson, J.M., Gorham, B.E., Dragut, L.D., 2006. Using digital photographs and object-based image analysis to estimate percent ground cover in vegetation plots. Frontiers in Ecology and the Environment, 4(8), 408–413

Mui, A., Y. He & Q. Weng, 2015. An object-based approach to delineate wetlands across landscapes of varied disturbance with high spatial resolution satellite imagery. ISPRS Journal of Photogrammetry and Remote Sensing 109: 30–46. doi:10.1016/j.isprsjprs.2015.08.005

Olofsson, P., Foody, G.M., Herold, M., Stehman, S.V., Woodcock, C.E., Wulder, M.A., 2014. Good practices for estimating area and assessing accuracy of land change. Remote Sensing of Environment 148 (2014) 42–57. Doi:10.1016/j.rse.2014.02.015

Radoux, J., Bogaert, P., Fasbender, D. & Defourny, P., 2011. Thematic accuracy assessment of geographic object-based image classification. International Journal of Geographical Information Science, 25:6, 895-911, DOI: 10.1080/13658816.2010.498378Rampi, L. P., J. F. Knight & K. C. Pelletier, 2014. Wetland Mapping in the Upper Midwest United States. Photogrammetric Engineering & Remote Sensing 80, 439–448. doi:10.14358/PERS.80.5.439

Roelfsema, C.M., M. Lyons, E.M. Kovacs, P. Maxwell, M.I. Saunders, J. Samper-Villarreal & S.R. Phinn, 2014. Multi-temporal mapping of seagrass cover, species and biomass: A semi-automated object based image analysis approach. Remote Sensing of Environment 150: 172–187. doi:10.1016/j.rse.2014.05.001

Tiede, D., S. Lang, D. Hölbling & P. Füreder, 2010 Transferability of OBIA rule sets for IDP camp analysis in Darfur. The International Archives of the Photogrammetry, Remote Sensing and Spatial Information Sciences, XXXVIII-4/C7.

Tiede, D., S. Lang, F. Albrecht & D. Hölbling, 2010. Object-based Class Modeling for Cadastre-constrained Delineation of Geo-objects. Photogrammetric Engineering & Remote Sensing 76: 193–202. doi:10.14358/PERS.76.2.193

Verhoeven, G., 2008. Imaging the invisible using modified digital still cameras for straightforward and low-cost archaeological near-infrared photography. Journal of Archaeological Science 35: 3087–3100. doi:10.1016/j.jas.2008.06.012

Verhoeven, G.J.J., 2010. It's all about the format – unleashing the power of RAW aerial photography. International Journal of Remote Sensing 31: 2009–2042. doi:10.1080/01431160902929271

Verschoren, V., J. Schoelynck, K. Buis, F. Visser, P. Meire & S. Temmerman, This issue. Mapping the spatio-temporal distribution of aquatic vegetation at reach scale in lowland rivers using a digital cover photography technique. Hydrobiologia.

Visser, F., K. Buis, V.Verschoren & P. Meire, 2015. Depth Estimation of Submerged Aquatic Vegetation in clear water streams using low-altitude optical remote sensing. Sensors 15: 25287–25312. doi:10.3390/s151025287

Visser, F., C. Wallis & A. M. Sinnott, 2013. Optical remote sensing of submerged aquatic vegetation: Opportunities for shallow clearwater streams. Limnologica - Ecology and Management of Inland Waters 43: 388–398. doi:10.1016/j.limno.2013.05.005

Woodget, A.S., Carbonneau, P.C., Visser, F. & Maddock, I., 2015. Quantifying submerged fluvial topography using hyperspatial resolution UAS imagery and structure from motion photogrammetry. Earth Surface Processes and Landforms 40: 47-64.

FIGURES

Fig. 1 Colour photo of *C. obtusangula* (l) and *R. peltatus* (r) patches. River flow direction is left to right. Despite the relatively similar leaf colour the plants can be distinguished due to variation in plant morphology

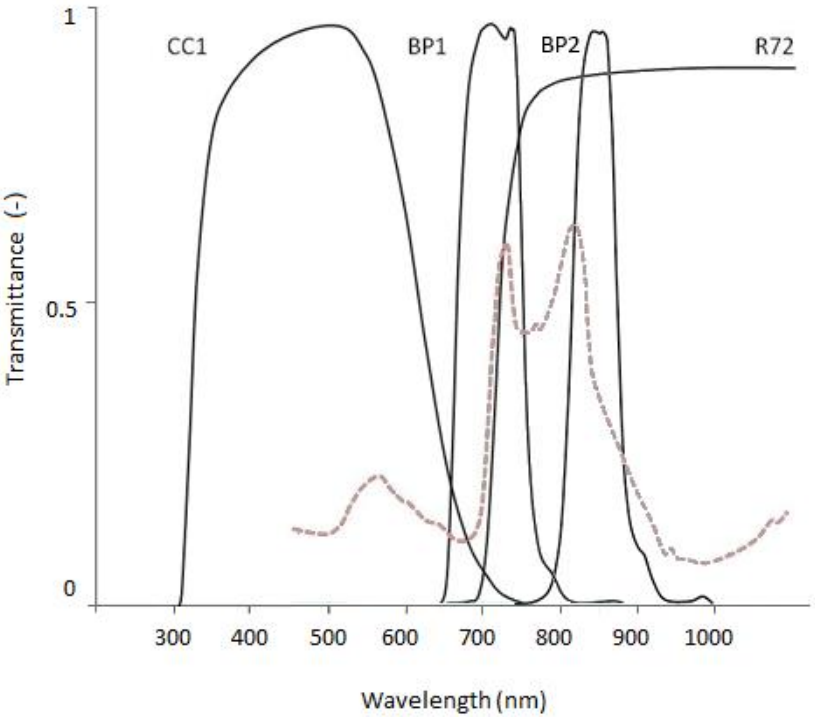

Fig. 2 Transmission spectra of NIR(BP1) and NIR(BP2) bandpass filters and CC1 and NIR(R72) blocking filters based on manufacturers specifications (maxmax.com). Submerged macrophyte spectrum included with dashed line for comparison (source: Visser et al., 2015)

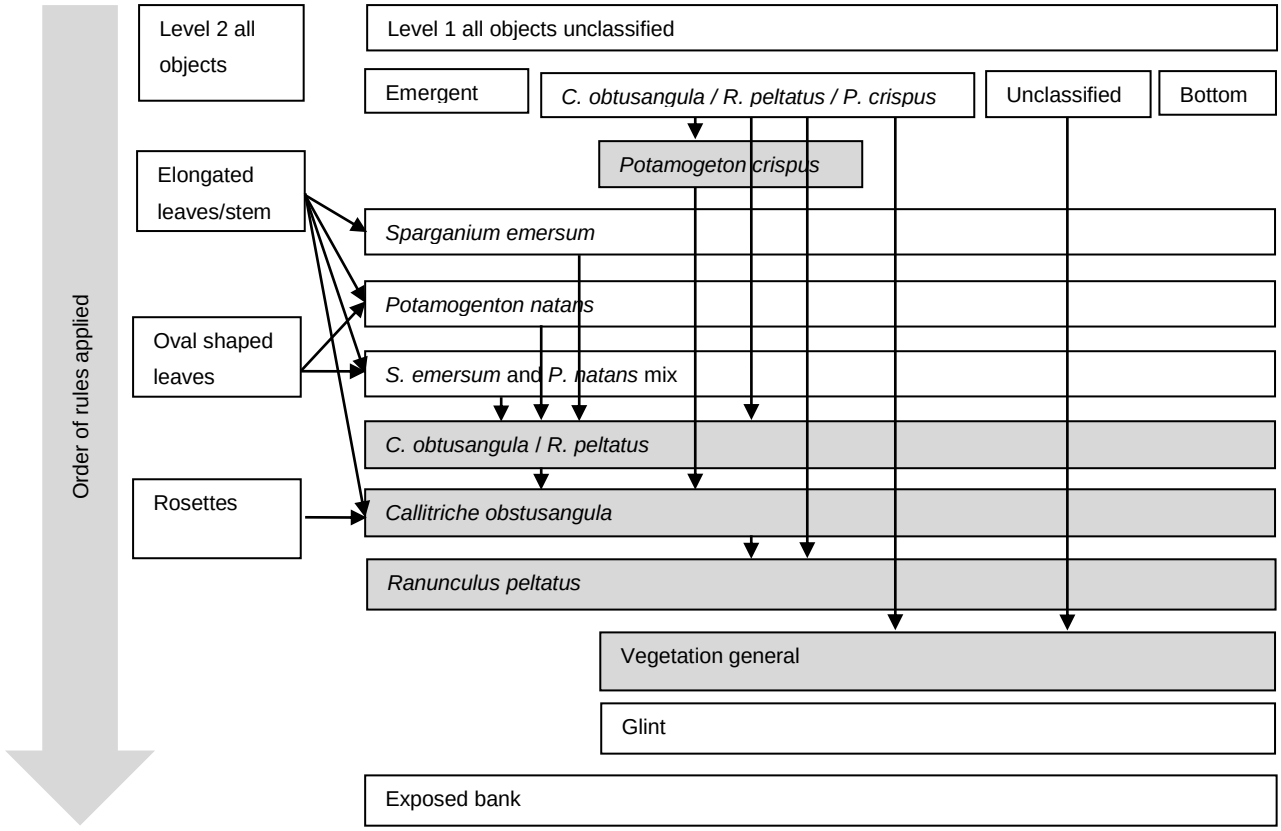

Fig. 3 Flow diagram illustrating the structure of the rule set used to classify objects into the designated classes. Classes shown in grey are created using objects from only a limited range of existing classes as input. These source classes are indicated with arrows. Classes shown in white were created using all objects in the classification process.

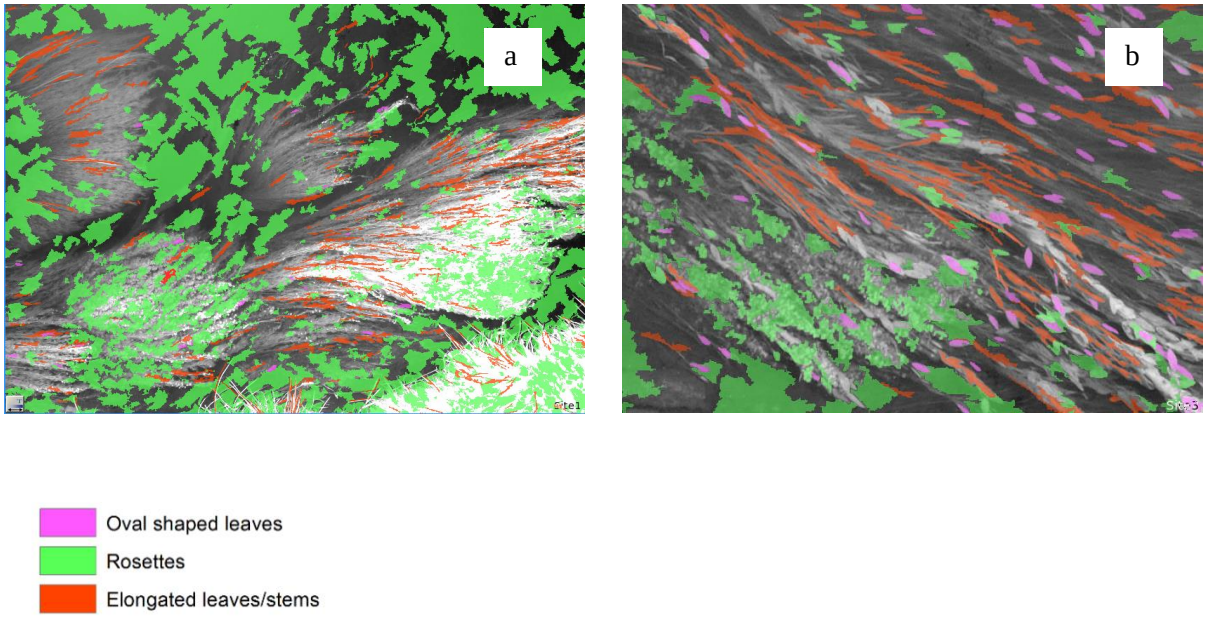

Fig. 4 Level 2 classification of site 1 showing Rosette objects (a and b), Elongated leaf/stem objects (a and b) and Oval shaped leaves (b)

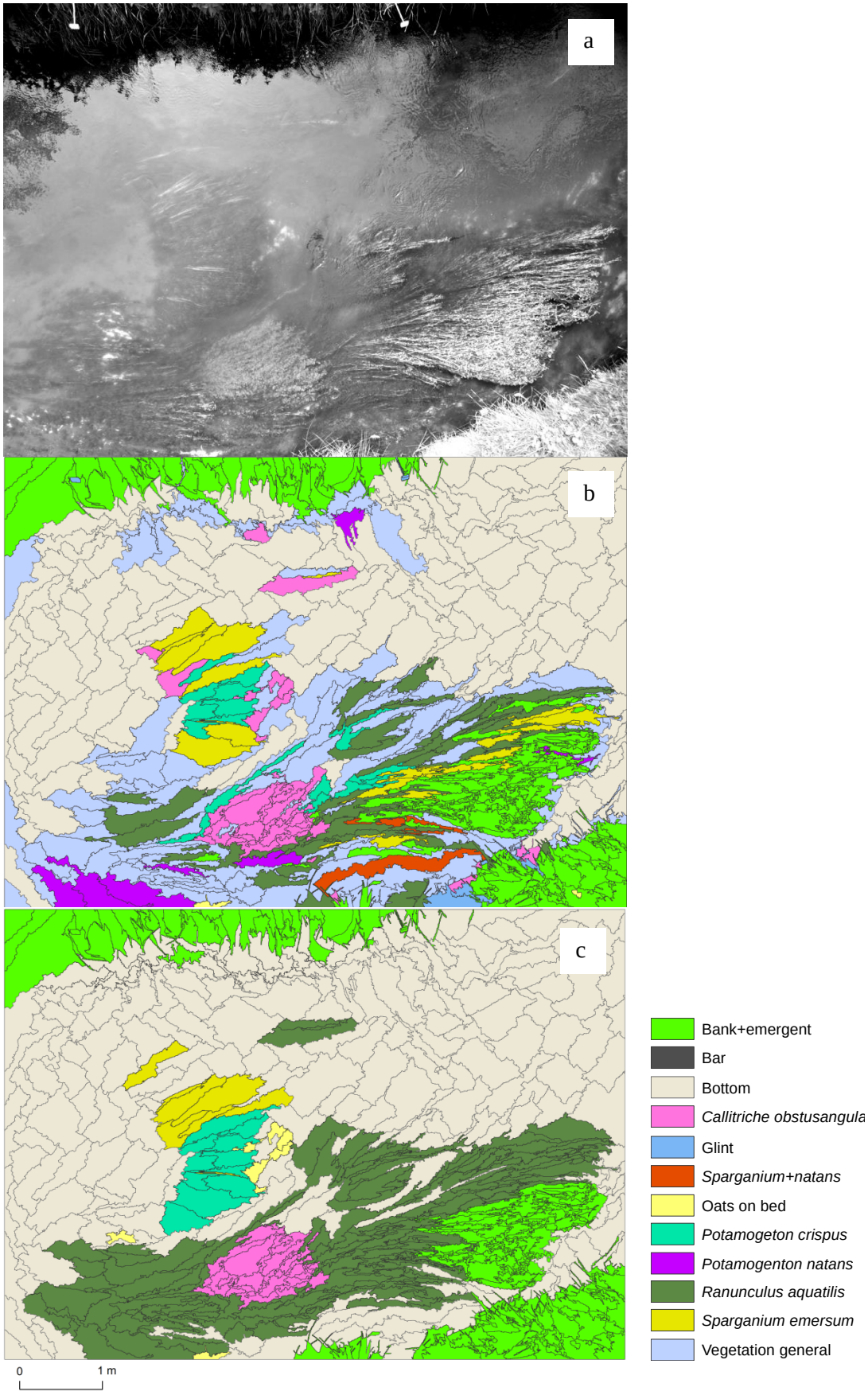

Fig. 5 Site 1 NIR(BP1) image (a), OBIA classification (b) and manual classification (c)

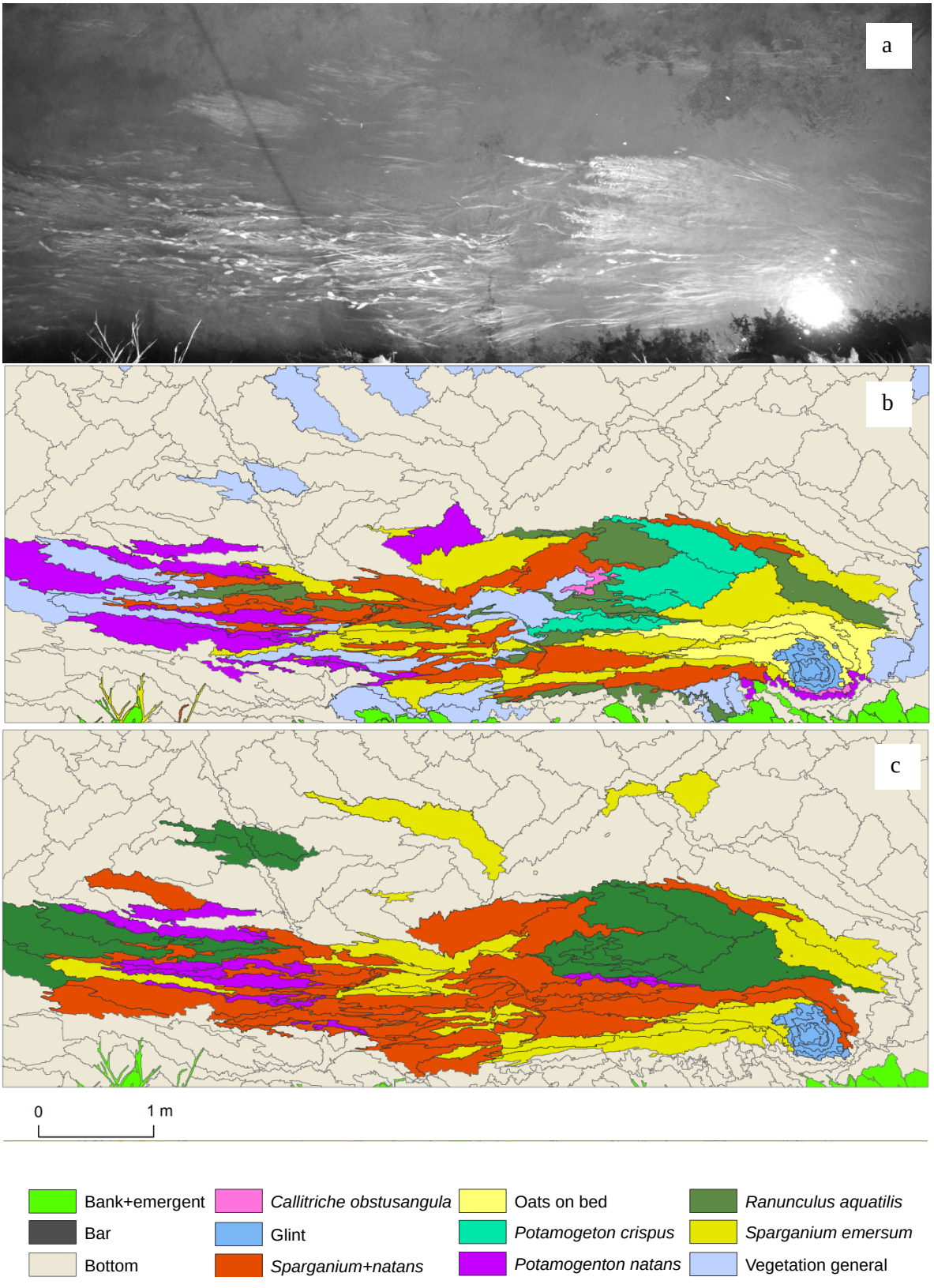

Fig. 6 Site 2 NIR(BP1) image (a), OBIA classification (b) and manual classification (c)

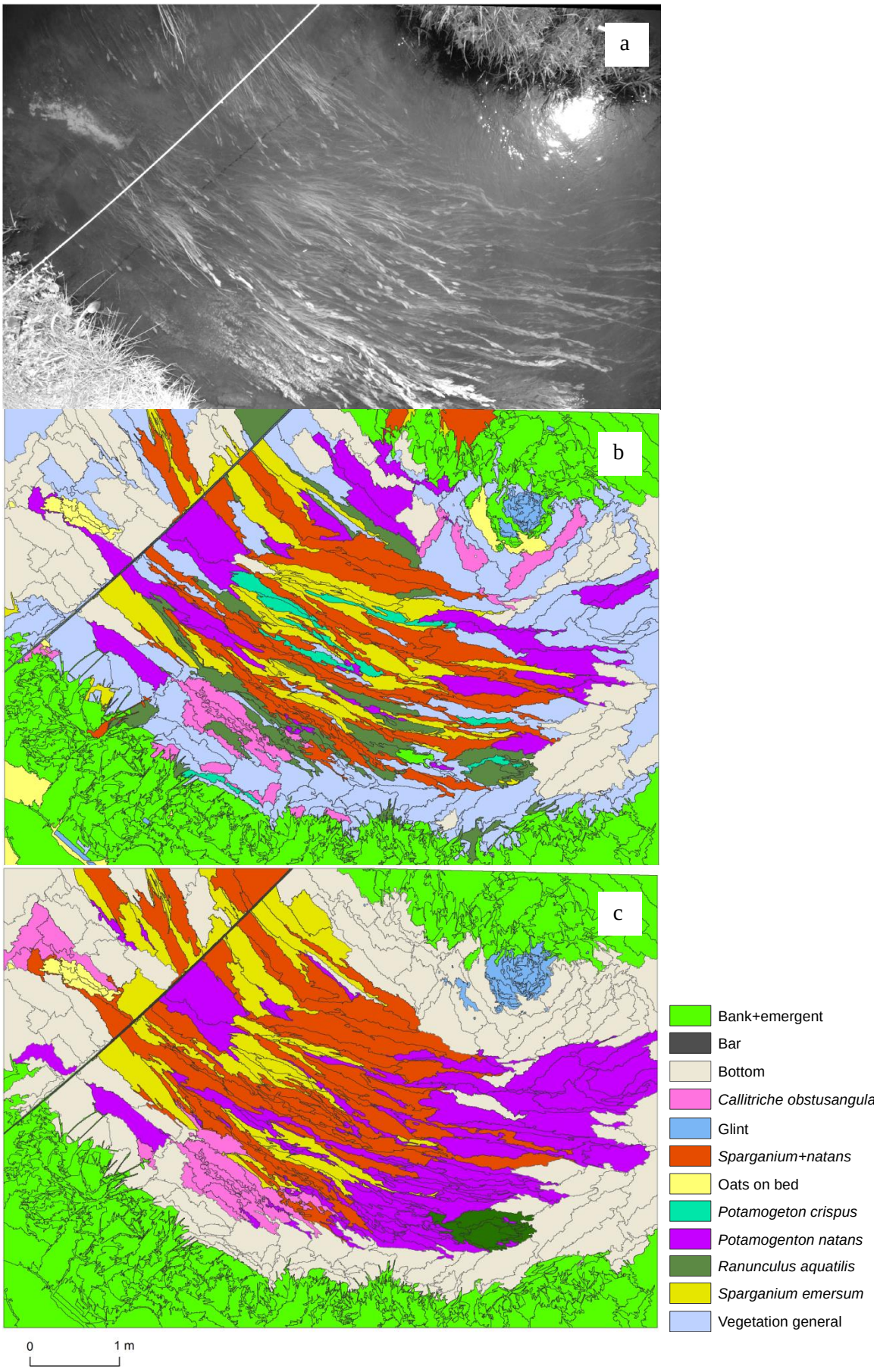

Fig. 7 Site 3 NIR(BP1) image (a), OBIA classification (b) and manual classification (c)

TABLES

Table 1 Rules and thresholds used to assign objects for all classes used. Classes including (f) are final classes as used on the final maps. Classes including (t) are intermediate classes used in the classification process. All classes were created at segmentation level 1, unless 'L2' is included indicating the class was created at Level 2. Rules marked with (*) rely on absolute reflectance values

Class name	Rules + thresholds applied
Bank/Emergent (f)	*Mean NIR(R72) > 160
	NDVI >= 0
Bottom (f)	*Mean NIR(BP2) < 35
	Standard deviation NIR(R72) < 4.5
C.obtusangula/*R.peltatus*/*P.crispus* (t)	*Mean NIR(BP1) > 65
C. obtusangula / R. peltatus (t)	Mean curvature/Length sub objects > 5.5
	Mean L/W ratio sub objects < 4
	*135 < Mean red < 155
Rosettes (L2, t)	Length/width ratio < 2
Elongated leaves/stems (L2, t)	Length/width > 1
	*Mean NIR(BP1) > 60
	Relative border to brighter objects NIR(BP1) < 0.5
	Width < 18 pxl
Oval shaped leaves (L2, t)	Area < 450 pxl
	90 < Brightness < 134
	Eliptic fit > 0.65
	Length < 50 pxl
	1.5 < Length/Width < 4
	Mean difference to neigbours NIR(BP1) > 6

	Roundness < 1.2
Callitriche obtusangula (f)	Number of elongated leaves/stems < 2
	Relative area of rosettes > 0.23
Sparganium emersum (f)	Mean curvature/Length sub objects < 5.4
	Number of oval shaped leaves <= 1
	Or
	Number of elongated leaves/stems > 2
	Relative area elongated leaves/stems > 0.4
Potamogeton natans (f)	Number of oval shaped leaves > 1
	Relative area elongated leaves/stems <= 0.4
P. natans and *S. emersum* mix (f)	Number of oval shaped leaves > 1
	Relative area of elongated leaves/stems > 0.4
	Or
	Number of elongated leaves/stems > 2
	Relative area elongated leaves/stems > 0.4
Ranunculus peltatus (f)	Number of elongated leaves/stems > 1
Potamogeton Crispus (f)	*3 < Standard deviation NIR(BP1) < 5.5
Vegetation general (f)	*Standard deviation NIR(BP2) > 3
Exposed bank (f)	*Mean Red > 190
Sunglint (f)	Brightness > 160
	NDVI < 0

Table 2 Accuracy values for the OBIA classifications compared to a manually delineated classification.

	Overall Accuracy (%)
Site 1	(304/496) =61

Site 2	(149/241) = 61
Site 3	(309/580) = 53

Table 3 Error matrices showing for each class the number of correctly classified polygons and the alternative class allocation of misclassified polygons, for sites 1 (a), 2 (b) and 3 (c)

a) Site 1 *Manual delineation:*

	Bank	Bottom	*C. obtusangula*	*P. crispus*	*S. emersum*	Glint	Mix	*P. natans*	Exposed	*R. peltatus*	Vegetation	Total	User'sacc.	Errors of commission
Classification:														
Bank	107	1	4	0	2	7	0	1	1	4	14	141	0.76	0.24
Bottom	5	140	2	0	1	0	1	2	0	3	50	204	0.69	0.31
C. obtusangula	1	0	13	0	0	0	0	0	0	0	3	17	0.76	0.24
P. crispus	0	0	0	7	3	0	0	0	0	0	1	11	0.64	0.36
S. emersum	0	1	1	1	4	0	0	0	0	0	1	8	0.50	0.50
Glint	0	0	0	0	0	0	0	0	0	0	0	0	-	-
Mix	0	0	0	0	0	0	0	0	0	0	0	0	-	-
P. natans	0	0	0	0	0	0	0	0	0	0	0	0	-	-
Exposed	0	0	3	0	0	0	0	0	1	0	1	5	0.20	0.80
R. peltatus	14	1	3	6	9	0	2	4	0	32	39	110	0.29	0.71
Vegetation	0	0	0	0	0	0	0	0	0	0	0	0	-	-
total	127	143	26	14	19	7	3	7	2	39	109	496		
Producer's acc.	0.84	0.98	0.50	0.50	0.21	0.00	0.00	0.00	0.50	0.82	0.00			
Errors of omission	0.16	0.02	0.50	0.50	0.79	1.00	1.00	1.00	0.50	0.18	1.00			

b) Site 2 *Manual delineation:*

	Bank	Bottom	*C. obtusangula*	*P. crispus*	*S. emersum*	Glint	Mix	*P. natans*	Exposed	*R. peltatus*	Vegetation	Total	User'sacc.	Errors of commission
Classification:														
Bank	16	0	0	0	2	0	2	0	0	0	0	20	0.8	0.2
Bottom	7	96	0	0	0	0	0	3	1	2	17	126	0.76	0.24
C. obtusangula	0	0	0	0	0	0	0	0	0	0	0	0	-	-
P. crispus	0	0	0	0	0	0	0	0	0	0	0	0	-	-
S. emersum	0	4	0	0	9	0	4	0	1	2	2	22	0.41	0.59
Glint	0	0	1	0	0	8	0	0	1	0	0	10	0.8	0.2

Mix	0	2	0	1	7	0	8	2	2	3	7	32	0.25	0.75
P. natans	0	0	0	1	1	0	1	7	0	1	1	12	0.58	0.42
Exposed	0	0	0	0	0	0	0	0	0	0	0	0	-	-
R. peltatus	0	2	1	3	1	0	1	1	0	5	5	19	0.26	0.74
Vegetation	0	0	0	0	0	0	0	0	0	0	0	0	-	-
total	23	104	2	5	20	8	16	13	5	13	32	241		
Producer's acc.	0.70	0.92	0	0	0.45	1	0.5	0.54	0	0.38	0			
Errors of omission	0.30	0.08	1	1	0.55	0	0.5	0.46	1	0.62	1			

c) Site 3 *Manual delineation:*

	Bank	Bottom	*C. obtusangula*	*P. crispus*	*S. emersum*	Glint	Mix	*P. natans*	Exposed	*R. peltatus*	Vegetation	Bar	Total	User'sacc.	Errors of commission
Classification:															
Bank	182	1	2	0	4	4	3	0	5	7	16	0	224	0.81	0.19
Bottom	2	35	7	1	0	0	0	4	2	1	67	0	119	0.29	0.71
C. obtusangula	0	2	8	0	0	0	0	0	0	4	3	0	17	0.47	0.53
P. crispus	0	0	0	0	0	0	0	0	0	0	0	0	0	-	-
S. emersum	0	6	0	2	17	0	1	0	0	4	6	0	36	0.47	0.53
Glint	11	11	0	0	0	11	0	1	4	0	1	0	39	0.28	0.72
Mix	0	3	0	3	9	0	23	3	0	5	4	0	50	0.46	0.54
P. natans	1	3	1	2	10	0	15	17	0	12	24	0	85	0.20	0.80
Exposed	0	0	0	0	0	0	0	0	4	0	0	0	4	1.00	0.00
R. peltatus	0	0	0	1	0	0	0	0	0	4	1	0	6	0.67	0.33
Vegetation	0	0	0	0	0	0	0	0	0	0	0	0	0	-	-
Bar	0	0	0	0	0	0	0	0	0	0	0	8	8	1.00	0.00
total	196	61	18	9	40	15	42	25	15	37	122	1.00	580		
Producer's acc.	0.93	0.57	0.44	0.00	0.43	0.73	0.55	0.68	0.27	0.11	0.00	0.00			
Errors of omission	0.07	0.43	0.56	1.00	0.58	0.27	0.45	0.32	0.73	0.89	1.00	0.00			